Journal of Sol-Gel Science and Technology (2018) 88:639–645
https://doi.org/10.1007/s10971-018-4864-y

ORIGINAL PAPER: SOL-GEL AND HYBRID MATERIALS FOR DIELECTRIC, ELECTRONIC, MAGNETIC AND FERROELECTRIC APPLICATIONS

Preparation of epitaxial $CaMn_7O_{12}$ film via sol-gel method and its ferromagnetic properties

Yunwei Wang[1,2] · Gaoyang Zhao[1] · Chuanbao Wu[3] · Zongfan Duan[1]

Received: 10 August 2018 / Accepted: 24 October 2018 / Published online: 3 November 2018

Abstract

$CaMn_7O_{12}$ precursor sol was prepared by using $Ca(NO_3)_2{\cdot}4H_2O$ and $Mn(CH_3COO)_4{\cdot}4H_2O$ as the raw materials, acetylacetone (AcAcH) as the chelating agent, and methyl alcohol (MeOH) as the solvent. The $CaMn_7O_{12}$ crystalline film was obtained via dip-coating and annealing treatment on the $LaAlO_3$ (001) single-crystal substrate. XRD θ-2θ scan indicated that the as-prepared $CaMn_7O_{12}$ film had strong preferred orientation along the *c*-axis. In addition, the results of the ω and ϕ scans demonstrated that the film exhibited outstanding out-of-plane and in-plane texture characteristics. The SEM characterization showed that the $CaMn_7O_{12}$ film was dense and free of cracks. The grain size was uniform with an average size of ~180 nm. Vibrating sample magnetometer (VSM) test results indicated the $CaMn_7O_{12}$ film was antiferromagnetic and had a saturation magnetization of 114.2 emu/cm^3 at 50 K.

Graphical Abstract

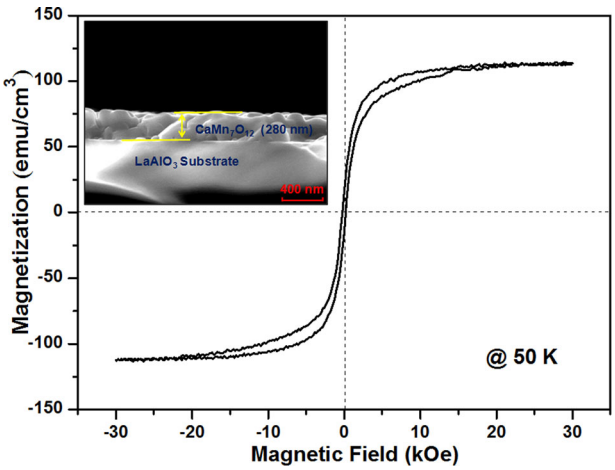

✉ Gaoyang Zhao
zhaogy@xaut.edu.cn

✉ Zongfan Duan
duanzf@xaut.edu.cn

[1] School of Materials Science and Engineering, Xi'an University of Technology, 710048 Xi'an, China

[2] School of Biological and Chemical Engineering, Panzhihua University, 617000 Panzhihua, China

[3] College of Vanadium and Titanium, Panzhihua University, 617000 Panzhihua, China

Highlights

- A $CaMn_7O_{12}$ film was deposited on (001) $LaAlO_3$ substrate by sol-gel method.
- The as-prepared film exhibited good out-of-plane and in-plane texture characteristics.
- The film was antiferromagnetic and had a saturation magnetization of 114.2 emu/cm^3 at 50 K.

Keywords $CaMn_7O_{12}$ · Thin film · Epitaxy · Sol-gel method · Magnetic properties · Multiferroic materials

1 Introduction

Single-phase multiferroic materials possess both ferroelectric and ferromagnetic orders, resulting in the magnetoelectric effect. These materials have been successfully employed in the fields of spintronics, multi-state storage devices, and micro electro mechanical system [1–3]. According to the microscopic origin of ferroelectricity, Khomskii et al. classified single-phase multiferroics into two types [4, 5]. In the Type I multiferroics, such as $BiFeO_3$, ferroelectricity and magnetism have different origins. This type of materials often presents high critical temperature and polarizations; however, the coupling between ferroelectricity and magnetism is relatively weak, which is a disadvantage to the practical application [6, 7]. In the Type II multiferroics, such as $CaMn_7O_{12}$, the ferroelectricity is induced by a particular magnetic order. Because of the magnetically induced ferroelectric mechanism, the intrinsic magnetoelectric effect is strong; therefore, a series of new functions can be developed through the synergistic effect of ferroelectricity. Owing to their outstanding properties, Type II multiferroic materials have attracted considerable attention [8].

Dong et al. experimentally assessed the magnetically induced multiferroic properties of $CaMn_7O_{12}$, and measured its magnetic phase transition (~90 K) [9]. Then, the ferroelectric polarization of the single crystalline $CaMn_7O_{12}$ was measured by Johnson et al. to be 2870 μC/m^2 [10], which was the highest magnetic multiferroic polarization observed in the bulk material system at that time. The ferroelectricity of $CaMn_7O_{12}$ is caused by the propeller-like magnetic order structure, i.e., the spontaneous polarization is caused by the magnetic structure [11]. Because of the presence of a weak Jahn–Teller distortion, strong Dzyaloshinskii–Moria interaction (which control the direction of the polarization), and the simultaneous exchange striction (which increases the polarization) in $CaMn_7O_{12}$, its intrinsic magnetoelectric coupling is strong [9]. These works on $CaMn_7O_{12}$ not only provide additional insights into the design of next-generation multi-functional electronic devices but also significantly expand the research scope of multiferroic materials. It will provide a huge driving force for the development of new information storage-processing magnetoelectric devices based on magnetic-ferroelectric coupling effect [12–14].

Previous studies focused on the properties of bulk $CaMn_7O_{12}$, by taking advantage of first-principle calculations and density functional theory; nevertheless, little research on $CaMn_7O_{12}$ films has been reported. However, the thin film is an essential form for magnetoelectric devices fabrication. Until 2015, Huon et al. deposited $CaMn_7O_{12}$ films with *c*-axis orientation on $SrLaAlO_4$ and $La_{0.3}Sr_{0.7}Al_{0.65}Ta_{0.35}O_3$ substrates via the oxide molecular beam epitaxy method. They studied the changes of the film resistivity along with the temperature and determined the phase transition temperature. Nonetheless, the corresponding ferromagnetic properties are still lacking [15]. The high-vacuum condition is required for physical methods, such as the molecular beam epitaxy method, whereas the equipment is expensive, thus not suitable for mass production. The cost of the sol-gel method is low, and its composition is easy to controls; therefore, this method can be applied to large-scale industry. In this work, we prepared a $CaMn_7O_{12}$ film on $LaAlO_3$ (001) single-crystal substrate via the sol-gel method and investigated its biaxial texture characteristics and magnetic properties.

2 Experimental detail

2.1 Materials

All reagents of metallic salts and organic solvent were of analytic grade, and were purchased from Aladdin. They were used directly without further purification. A $LaAlO_3$ (001) substrate was purchased from Hefei crystal material Technology Co Ltd. It was cut into chips with the dimensions of 1 cm × 2 cm and then used as substrates to deposit $CaMn_7O_{12}$ films.

2.2 Preparation of $CaMn_7O_{12}$ films

$Ca(NO_3)_2{\cdot}4H_2O$ and $Mn(CH_3COO)_4{\cdot}4H_2O$ were chosen as the precursors. Anhydrous MeOH was the solvent, whereas acetylacetone (AcAcH) was the chelating agent. The $CaMn_7O_{12}$ sol was prepared with the metal ion proportion of Ca:Mn = 1:7. The preparation process is illustrated in Fig. 1. First, the solution A was obtained by dissolving 0.1771 g of $Ca(NO_3)_2{\cdot}4H_2O$ into 5 ml of MeOH. Afterward, 1.2867 g of $Mn(CH_3COO)_4{\cdot}4H_2O$ was dissolved into 5 ml

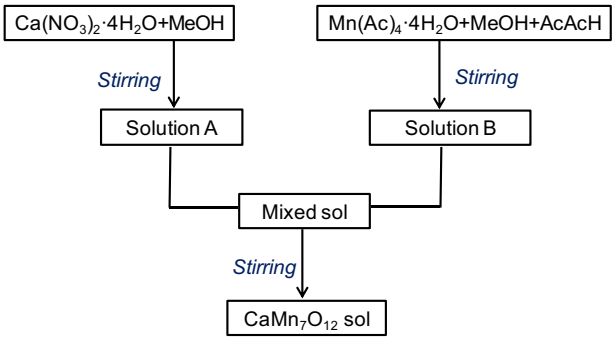

Fig. 1 Scheme of the preparation of the $CaMn_7O_{12}$ film

of MeOH; thus, 0.53 g of AcAcH was added. After stirring and clarifying, the solution B was obtained. The $CaMn_7O_{12}$ sol was obtained by mixing the solutions A and B. By supplementing proper amount of MeOH, the concentration of total metal ions was adjusted to 0.4 mol·L^{-1}. Finally, a stable and uniform $CaMn_7O_{12}$ sol was obtained after stirring for 24 h. The $CaMn_7O_{12}$ gel films were deposited on the $LaAlO_3$ (001) substrate via the dip-coating technique with a drawing rate of 1.0 mm/s. Subsequently, the coated $CaMn_7O_{12}$ gel films were annealed in air at 350 °C to eliminate any organic components. A proper thickness of the film was achieved by repeating the process of dip-coating and annealing for six times. Finally, the crystalline $CaMn_7O_{12}$ films were obtained after a re-annealing treatment at 730 °C for 90 min.

2.3 Characterization

A SmartLab X-ray diffractometer in θ-2θ, ω, and ϕ scan modes was used to determine the film phase, the out-of-plane texture, and the in-plane texture, respectively. Scanning electron microscopy (SEM) experiments were performed on a JEM-6700F after depositing conductive Pt onto the surface of the films. The chemical composition of the film was determined by energy dispersive X-ray spectrometry (EDS), and chemical state of ions was characterized via X-ray photoelectron spectroscopy (XPS) with Al Kα (1486.71 eV) line at a power of 150 W (10 mA, 15 kV). All the binding energies obtained in the XPS analysis were referenced to the C1s peak at 284.80 eV of the surface adventitious carbon. Magnetic measurements were performed with a vibrating sample magnetometer (VSM) in a physical property measurement system (Versalab, Quan-tum Design).

3 Results and discussion

3.1 Phase and orientation of the $CaMn_7O_{12}$ film

The $CaMn_7O_{12}$ film was prepared on $LaAlO_3$ (001) substrate. The XRD results are shown in Fig. 2. $CaMn_7O_{12}$ has

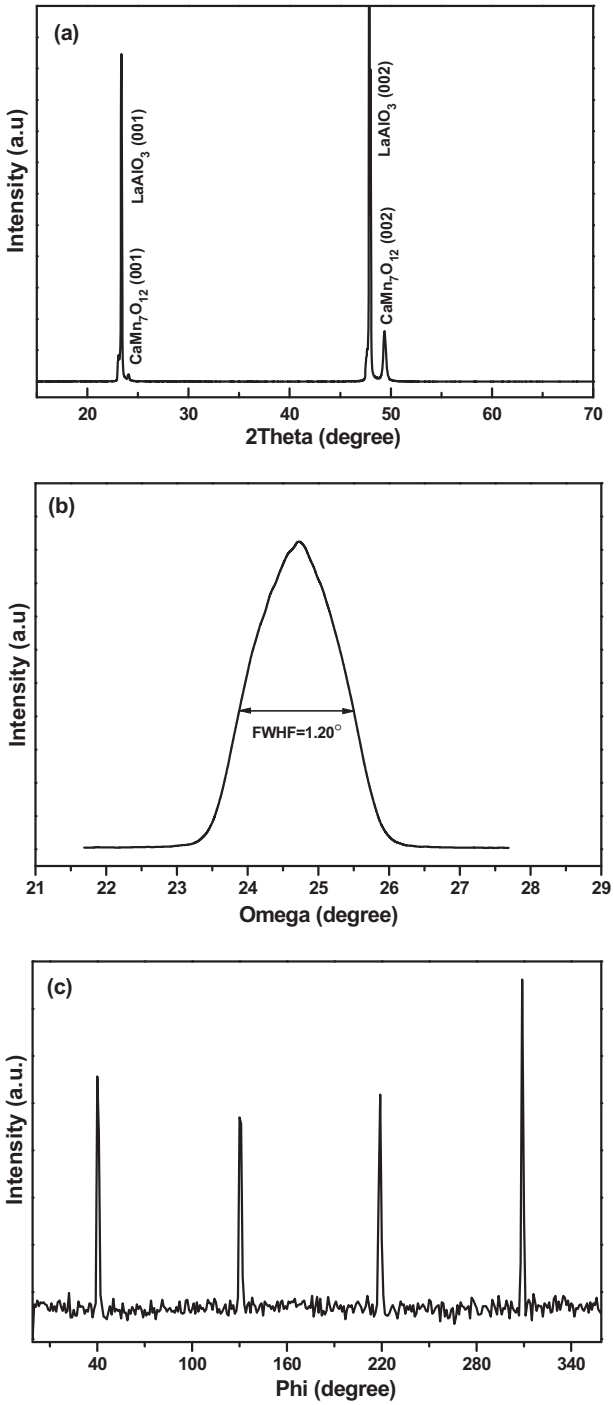

Fig. 2 XRD patterns of the $CaMn_7O_{12}$ film deposited on the $LaAlO_3$ substrate: **a** θ-2θ *scan*, **b** (002) ω-scan, and **c** (011) ϕ-scan

a pseudo-cubic structure with a lattice parameter of 3.682 Å. The crystal-lattice mismatch with $LaAlO_3$ (3.789 Å) substrate is only 2.9% [15, 16]. Therefore, it is possible to make the $CaMn_7O_{12}$ film growing epitaxially on the $LaAlO_3$ substrate. Figure 2(a) presents the XRD θ-2θ scanning results. It can be seen that, except the diffraction peaks of (001) and (002) from $LaAlO_3$, the peaks at $2\theta = 24.09°$ and

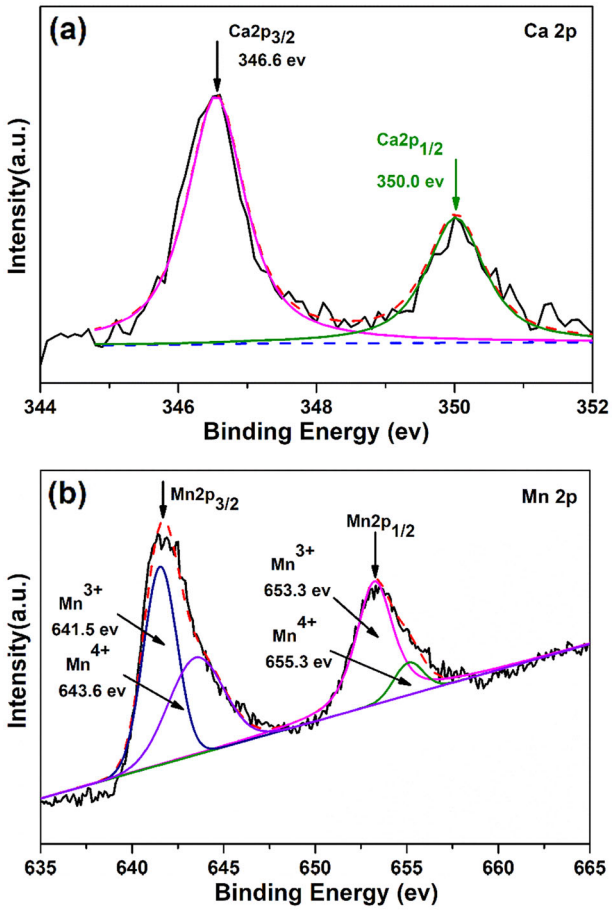

Fig. 3 XPS spectra of the $CaMn_7O_{12}$ film: high-resolution spectra of **a** Ca 2p and **b** Mn 2p

49.38° correspond to the $CaMn_7O_{12}$ crystal planes of (001) and (002). This indicates that the as-prepared $CaMn_7O_{12}$ film has strong preferred orientation along the *c*-axis, which is in agreement with the results obtained by A. Huon et al. via the molecular beam epitaxy method [15].

To further characterize the in-plane and out-of-plane textures of the $CaMn_7O_{12}$ film, ω and ϕ scanning tests were conducted on the (002) and (011) planes, as shown in Fig. 2 (b), (c), respectively. In the ω scan, the full-width at half-maximum (FWHM) of the $CaMn_7O_{12}$ (002) plane was 1.20°, indicating that the prepared $CaMn_7O_{12}$ film possessed outstanding out-of-plane texture characteristics. During the ϕ scan process, the sample was tilted at 45.15° first; then, the test was conducted within the range of a 360° sample rotation. It can be found from the ϕ scan result in Fig. 2(c) that the diffraction peaks occurred with 90° intervals are in accordance with the rotational symmetry of the pseudo-cubic structure. The average FWHM of the four peaks was 1.90°, which demonstrates that the $CaMn_7O_{12}$ film has good in-plane texture characteristics as well. Based on the XRD results, the as-prepared $CaMn_7O_{12}$ film has biaxial texture characteristics, which further confirms that $CaMn_7O_{12}$ film grew on $LaAlO_3$ substrate in epitaxial mode [17].

3.2 XPS measurement of the $CaMn_7O_{12}$ film

XPS is an excellent technique to determine the valence states of the samples. Thus, in this study, XPS was employed to analyze the valence states of the $CaMn_7O_{12}$ film (Fig. 3). XPS peak fitting and background subtraction were conducted using the XPS-PEAK4.1 software. From Fig. 3(a), it can be observed that there are two peaks at the binding energy positions of 346.6 eV and 350.0 eV, which correspond to $2p_{3/2}$ and $2p_{1/2}$ of Ca^{2+}, respectively, indicating that Ca is bivalent [18–22]. According to the high-resolution spectrum of Mn, shoulder peaks appear near the two main peaks. Through the peak-fit process, two peaks can be obtained at the binding energies of 641.5 eV and 643.6 eV, which correspond to the $2p_{3/2}$ paeks of trivalent and quadrivalent Mn, respectively. In addition, there are two peaks located at the binding energies of 653.3 eV and 655.3 eV, corresponding to the $2p_{1/2}$ peaks of trivalent and quadrivalent Mn, respectively. It, thus, indicates the Mn element in the $CaMn_7O_{12}$ film is in the mixed valence state of trivalence and quadrivalence [23–26].

3.3 Morphology of the $CaMn_7O_{12}$ film

Figure 4 shows the SEM morphology of the $CaMn_7O_{12}$ film. According to Fig. 4(a), the thickness of the film is about 280 nm. From Fig. 4(b), it can be seen that the film is dense and free of cracks. The grain size is uniform, whereas the average size is ~180 nm. The EDS spectra acquired from the $CaMn_7O_{12}$ film were examined and the results were shown in Fig. 4(c). Beside the peaks attributed to La and Al of $LaAlO_3$ substrate and Pt of conductive layer, the peaks of Ca and Mn were observed. The atomic rations of Ca:Mn is 1:7.4, which is closed to the stoichiometry (1:7.0) of the nominal chemical composition of $CaMn_7O_{12}$. This indicates that the chemical component of the as-prepared film is relative appropriate.

3.4 Magnetism of the $CaMn_7O_{12}$ film

$CaMn_7O_{12}$ belongs to perovskite materials and has antiferromagnetic characteristics at low temperature. Although the magnetic property of bulk $CaMn_7O_{12}$ has been reported, that of $CaMn_7O_{12}$ films has not been studied yet. Figure 5 shows the hysteresis loop of the $CaMn_7O_{12}$ film deposited on the $LaAlO_3$ substrate at 50 K. The external magnetic field was in the range of −30 kOe to 30 kOe, which was perpendicular to the surface plane of the film. From Fig. 5, it can be seen that the $CaMn_7O_{12}$ film exhibits evident antiferromagnetic properties. It has a saturation magnetization

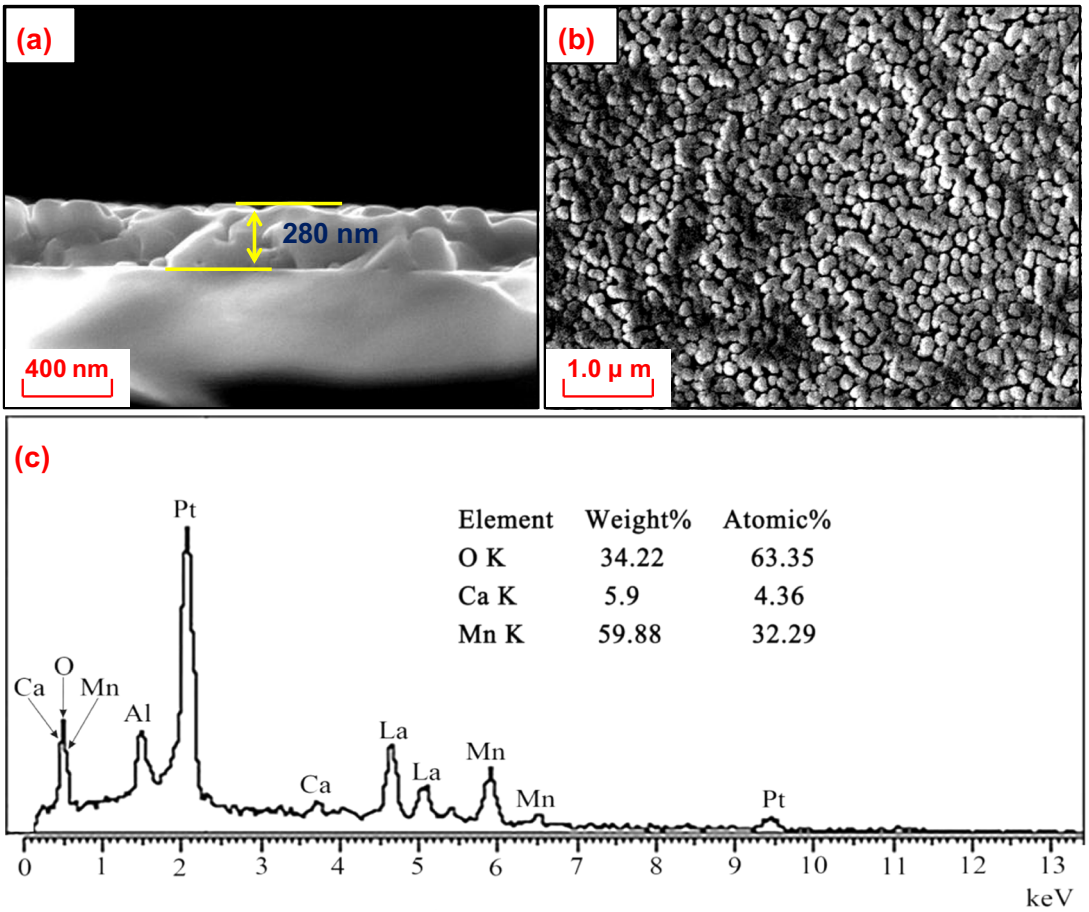

Fig. 4 SEM images and EDS spectra of $CaMn_7O_{12}$ film: **a** Cross-section image, **b** Surface morphology image, and **c** EDS spectra

of 114.2 emu/cm^3, a residual magnetization of 15.4 emu/cm^3, and a coercivity of 220 Oe. As measured by Jaiswar S et al., the saturation magnetization of the polycrystalline $CaMn_7O_{12}$ bulk material is ~10 emu/g under a magnetic field of 30 kOe at 50 K [18]. According to the density of $CaMn_7O_{12}$ of 5.107 g/cm^3, as found in PDF card 26-1114, the saturation magnetization of the bulk polycrystalline $CaMn_7O_{12}$ is 51.07 emu/cm^3. Therefore, the saturation magnetization of the $CaMn_7O_{12}$ film is higher than that of polycrystalline bulk materials, which is correlated to the highly biaxial textured characteristics of the as-prepared film. Compared with the bulk $CaMn_7O_{12}$, the as-prepared $CaMn_7O_{12}$ film exhibited improved ferromagnetic properties. It might be attributed to two causes. Firstly, it is probably attributed to the size effect of nanostructures in the thin film. It is well known that there is a cycloid structure in the bulk, which can restrict the release of magnetic properties. While, for $CaMn_7O_{12}$ thin film, the cycloid structure is partially broken down and then leads to better ferromagnetic properties [27–29]. Furthermore, strain effect might be the other primary reason. Several reports have indicated that the saturated magnetism of the highly strained

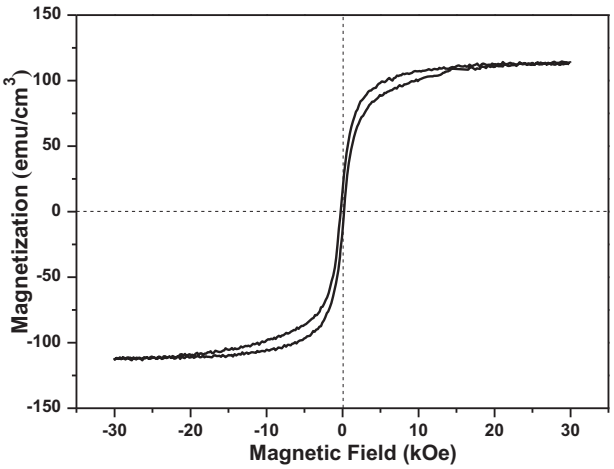

Fig. 5 Hysteresis loop of the $CaMn_7O_{12}$ film measured at 50 K

phase in multiferroic materials are about several times larger than that of the relaxed one [6, 30]. As mentioned above, the lattice constants of $CaMn_7O_{12}$ and $LaAlO_3$ are 3.682 and 3.789 Å, respectively. It makes the $CaMn_7O_{12}$

feromagnetic phase suffer a compressive strain, resulting in the enhancement of ferromagnetic properties.

It is well known that the easy magnetization axis of the $CaMn_7O_{12}$ is along *c*-axis direction [31, 32]. For $CaMn_7O_{12}$ film, the epitaxial growth on *c*-axis orientated $LaAlO_3$ substrate will be beneficial to improve its ferromagnetic properties. Furthermore, in epitaxial ferromagnetic film, the epitaxial constraint can induce a transition between cycloidal and homogeneous antiferromagnetic spin states which can release a latent antiferromagnetic component locked within the cycloid via magnetoelectric exchange. As a result, an enhanced magnetization value can be obtained in epitaxial ferromagnetic film [29]. Thus, the highly biaxial textured characteristics of as-prepared $CaMn_7O_{12}$ film make it exhibit excellent ferromagnetism.

4 Conclusions

The $CaMn_7O_{12}$ film was prepared via sol-gel process on $LaAlO_3$ (001) single-crystal substrate. The crystalline structure, phase composition, and elemental valence state were determined via XRD, SEM, and XPS techniques, respectively. Our results indicated that the as-prepared film was characterized by a perovskite structure with a dense surface, uniform grain size, and with an average grain size of ~180 nm. In addition, ω and ϕ scan tests demonstrated that the $CaMn_7O_{12}$ film exhibited good biaxial texture properties, leading to a saturation magnetization value of 114.2 emu/cm^3 at 50 K, which was notably higher than the reported value of the magnetization of the polycrystalline $CaMn_7O_{12}$ bulk materials.

Acknowledgements This work was supported by the project of the National Natural Science Foundation of China (51672212), the Scientific Research Fund (2013JK0676) of the Department of Education and Nature Science Foundation (2018JM5019) of Shaanxi Province, Panzhihua Science and Technology Program (2017CY-G-18) of Sichuan province, and Doctoral Fund (bkqj2017009) and student innovation and entrepreneurship training project (2018cxcy093) of Panzhihua University.

Conflict of interest The authors declare that they have no conflict of interest.

References

1. Schmid H (1994) Multi-ferroic magnetoelecrics. Ferroelectrics 162:317–338
2. Lim JS, Saldana-Greco D, Rappe AM (2018) Improper magnetic ferroelectricity of nearly pure electronic nature in helicoidal spiral $CaMn_7O_{12}$. Phys Rev B 97:045115
3. Lu XZ, Whangbo M-H, Dong S, Gong XG, Xiang HJ (2012) Giant ferroelectric polarization of $CaMn_7O_{12}$ induced by a combined effect of Dzyaloshinskii–Moriya interaction and exchange striction. Phys Rev Lett 108:187204
4. Kimura T, Goto T, Shintani H, Ishizaka K, Arima T, Tokura Y (2003) Magnetic control of ferroelectric polarization. Nature 426:55–58
5. Khomskii D (2009) Trend: classifying multiferroics: mechanisms and effects. Physics 2:20
6. Lu CL, Hu WJ, Tian YF, Wu T (2015) Multiferroic oxide thin film and heterostructures. Appl Phys Rev 2:021304
7. Spaldin NA, Fiebig M, Mostovoy M (2008) The toroidal moment in condensed-matter physics and its relation to the magnetoelectric effect. J Phys-Condens Mat 20:434203
8. Dong S, Liu JM (2012) Recent progress of multiferroic perovskite manganites. Mod Phys Lett B 26:1320004
9. Zhang GQ, Dong S, Yan ZB, Guo YY, Zhang QF, Yunoki S, Dagotto E, Liu JM (2011) Multiferroic properties of $CaMn_7O_{12}$. Phys Rev B 84:174413
10. Johnson RD, Chapon LC, Khalyavin DD, Manuel P, Radaelli PG, Martin C (2012) Giant improper ferroelectricity in ferroaxial magnet $CaMn_7O_{12}$. Phys Rev Lett 108:067201
11. Dai JQ (2017) Dependence of improper ferroelectricity on the preferred orientation of Mn3 spins in $CaMn_7O_{12}$. J Magn Magn Mater 424:314–322
12. Zhang HG, Ma XC, Xie L (2015) The structural and magnetic properties of Sr-doped multiferroic $CaMn_7O_{12}$. Int J Mod Phys B 29:1550221
13. Zhang JT, Lu XM, Zhou J, Sun H, Huang FZ, Zhu JS (2013) Magnetic properties and origins of ferroelectric polarization in multiferrioic $CaMn_7O_{12}$. Phys Rev B 87:075127
14. Gautam K, Shukla DK, Francoual S, Bednarcik J, Mardegan JRL, Liermann H-P, Sankar R, Chou FC, Phase DM, Strempfer J (2017) Large negative thermal expansion in the cubic phase $CaMn_7O_{12}$. Phys Rev B 95:144112
15. Huon A, Lang AC, Saldana-Greco D, Lim JS, Moon EJ, Rappe AM, Taheri ML, May SJ (2015) Electronic transition above room temperature in $CaMn_7O_{12}$ films. Appl Phys Lett 107:142901
16. Slawinkski S, Przenioslo R, Sosowska I, Petricek V (2012) Helical screw type magnetic structure of the multiferroic $CaMn_7O_{12}$ with low Cu-doping. Acta Cryst B68:240–249
17. Duan Z, Cui Y, Shi X, Wei J, Ren P, Zhao G (2016) Facile fabrication of micro-patterned LSMO films with unchanged magnetic properties by photosensitive sol-gel method on $LaAlO_3$ substrates. Ceram Int 42:141000–14106
18. Jaiswar S, Mandal KD (2017) Evidence of enhanced oxygen vacancy defects inducing ferromagnetism in multiferroic $CaMn_7O_{12}$ manganite with sintering time. J Phys Chem C 121:19586–19601
19. Kou J, Xu S, Sun T, Sun C, Guo Y, Wang C (2016) A study of sodium oleate adsorption on Ca^{2+} activated quartz surface using quartz crystal microbalance with dissipation. Int J Miner Process 154:24–34
20. Hanawa T, Ota M (1992) Characterization of surface film formed on titanium in electrolyte using XPS. Appl Surf Sci 55:269–276
21. Zhou F, Feng X, Yu J, Jiang X (2018) High performance of 3D porous graphene/lignin/sodium alginate composite for adsorption of Cd(II) and Pb(II). Environ Sci Pollut R 25:15651–15661
22. Qing Du, Wei D, Liu S, Cheng S, Hu N, Wang Y, Li B, Jia D, Zhou Y (2018) The hydrothermal treated Zn-incorporated titania based microarc oxidationcoating: surface characteristics, apatite-inducing ability and antibacterial ability. Surf Coat Tech 352:489–500
23. Sannigrahi J, Chattopadhyay S, Dutta D, Giri S, Majumdar S (2013) Magnetic and electric properties of $CaMn_7O_{12}$ based multiferroic compounds: effect of electron doping. J Phys Condens Mat 25:246001

24. Beyreuther E, Grafström S, Eng LM (2006) XPS investigation of Mn valence in lanthanum manganite thin films under variation of oxygen content. Phys Rev B 73:155425
25. Gautam K, Shukla DK, Choudhary RJ, Phase DM (2017) Enroute to phase purity in $CaMn_7O_{12}$. AIP Conf Proc 1832:090041
26. Su Y, Li X, Ji H, Zhao Z, Zhang P (2018) Effect of Ca^{2+} and Mn^{2+} ions on the radiation properties of $LaAlO_3$. Ceram Int 44:20427–20431
27. Gao F, Chen XY, Yin KB, Dong S, Ren ZF, Yuan F, Yu T, Zou ZG, Liu J-M (2007) Visible-light photocatalytic properties of weak magnetic $BiFeO_3$ nanoparticles Adv Mater 19:2889–2892
28. Zhang ST, Lu MH, Wu D, Chen YF, Ming NB (2005) Larger polarization and weak ferromagnetism in quenched $BiFeO_3$ ceramics with a distorted rhombohedral crystal structure. Appl Phys Lett 87:262907
29. Bai F, Wang J, Wuttig M, Li J, Wang N, Pyatakov AP, Zvezdin AK, Cross LE, Viehland D (2005) Destruction of spin cycloid in $(111)_c$-oriented $BiFeO_3$ thin films by epitiaxial constraint: enhanced polarization and release of latent magnetization. Appl Phys Lett 86:032511
30. Wang J, Neaton JB, Zheng H, Nagarajan V, Ogale SB, Liu B, Viehland D, Vaithyanathan V, Schlom DG, Waghmare UV, Spaldin NA, Rabe KM, Wuttig M, Ramesh R (2003) Epitaxial $BiFeO_3$ multiferroic thin film heterostructures. Science 299:1719
31. Tanaka M, Harbison JP, Park MC, Park YS, Shin T, Rothberg GM (1994) Epitaxial orientation and magnetic properties of MnAs thin films grown on (001) GaAs: template effects. Appl Phys Lett 65:1964–1966
32. Atiq S, Ko H-S, Siddiqi SA, Shin S-C (2008) Effect of epitaxy and lattice mismatch on saturation magnetization of γ′-Fe4N thin films. Appl Phys Lett 92:222507